The International Archives of the Photogrammetry, Remote Sensing and Spatial Information Sciences, Volume XLIX-B4-2026
XXV ISPRS Congress 2026 “From Imagery to Understanding”, Commission IV, 4–11 July 2026, Toronto, Canada

Benchmarking and assessment of image-based methods for particulate matter estimation: The AQpictures project

Afshin Moazzam[1], Daniele Oxoli[1], Maria Antonia Brovelli[1], Songnian Li[2], Francesco Pirotti[3], Shishuo Xu[4]

[1] Department of Civil and Environmental Engineering, Politecnico di Milano, Piazza Leonardo da Vinci 32, 20133 Milan, Italy - (afshin.moazzam, daniele.oxoli, maria.brovelli)@polimi.it
[2] Department of Civil Engineering, Toronto Metropolitan University, 350 Victoria Street, Toronto, ON M5B 2K3, Canada - snli@torontomu.ca
[3] Interdepartmental Research Center in Geomatics, Department of Land, Environment, Agriculture and Forestry, University of Padova, Via dell’Università 16, 35020 Legnaro, Italy – francesco.pirotti@unipd.it
[4] Beijing University of Civil Engineering and Architecture, 15 Yongyuan Road, Daxing District, Beijing 102616, China – xushishuo@bucea.edu.cn

Keywords: Air Quality Monitoring, Air Pollution, $PM_{2.5}$, Outdoor Image Analysis

Abstract

Fine particulate matter ($PM_{2.5}$) is a major air-quality and public-health concern, while conventional monitoring networks remain limited in coverage and costly to deploy and maintain. This work presents the AQpictures project, which investigates alternative low-cost monitoring approaches based on outdoor imagery, such as webcam photographs, for $PM_{2.5}$ estimation. Milan, Italy, is used as a testbed for the preliminary implementation and assessment of representative image-based $PM_{2.5}$ estimation methods reported in the literature. The study combines a literature review with an experimental benchmark using webcam images paired with ground-sensor $PM_{2.5}$ measurements and ancillary meteorological data. The review confirms that a growing range of image-based PM estimation methods is emerging, although reproducibility remains limited due to the scarce availability of openly shared datasets and source code. Three modelling strategies were implemented and tested: a physics-based approach, a machine-learning regression model, and a simple deep-learning network. The tested models exhibited notable limitations overall. Machine-learning regression achieved high in-sample performance ($R^2 > 0.94$) but generalised poorly to test data ($R^2 \approx 0.21$), while the other approaches showed generally low or inconsistent predictive performance. Overall, the results suggest that webcam-based $PM_{2.5}$ estimation can serve as a low-cost complementary approach; however, its reliability is strongly influenced by illumination conditions, dataset size, and modelling choices. These findings highlight the need for larger and more diverse training datasets, improved model robustness, and the development of standardised and openly accessible benchmarking frameworks.

1. Introduction

Fine particulate matter with an aerodynamic diameter of less than 2.5 μm, commonly referred to as $PM_{2.5}$, represents one of the foremost environmental threats to public health worldwide (Chen et al., 2022). Globally, ambient air pollution, driven substantially by $PM_{2.5}$ exposure, is responsible for approximately 4.2 million premature deaths per year (Yao et al., 2022). $PM_{2.5}$ contains a large number of different chemical species emitted from several sources (Sloss and Smith, 2000). Long-term exposure to $PM_{2.5}$ is associated with a wide range of cardiovascular and respiratory diseases, including chronic bronchitis, asthma, emphysema, ischemic heart disease, and lung cancer. The impacts of $PM_{2.5}$ extend beyond human health, influencing atmospheric processes such as cloud formation and precipitation (Wang et al., 2022). At the urban scale, high $PM_{2.5}$ concentrations contribute to persistent haze, reducing visibility and adversely affecting daily activities.

Conventional $PM_{2.5}$ monitoring relies on ground-based stations equipped with optical and/or filter-based gravimetric sensors (He et al., 2018). While these instruments deliver high-precision, policy-compliant measurements, their scalability and spatial coverage are limited by high procurement, installation, and operational costs (Yue et al., 2019). As a result, monitoring networks remain sparse, with individual stations typically representing air quality over areas of 1–3 km, which is insufficient to capture the pronounced spatial heterogeneity and non-linear variability of $PM_{2.5}$ in urban environments (Liu et al., 2016). Satellite observations provide an alternative by offering extensive spatial coverage; however, they often struggle to accurately estimate near-surface $PM_{2.5}$ due to the indirect nature of retrieval methods (Fowler et al., 2020). These limitations have motivated the development of complementary and innovative monitoring approaches. Several studies have demonstrated that visual features in outdoor images correlate with $PM_{2.5}$ concentrations (Wang et al., 2024). In this context, widely available imaging sources, such as webcams and other outdoor cameras, represent a promising alternative due to their broad spatial distribution and relatively low installation and maintenance costs. Image-based estimation exploits the fact that airborne fine particles alter light propagation in the atmosphere, leading to observable changes in scene appearance (see Figure 1). These optical effects can be quantified and used as proxies for $PM_{2.5}$ concentration through different modelling strategies.

Existing approaches can be broadly categorised into physics-based, data-driven, and hybrid methods. Physics-based models rely on atmospheric optics to relate image properties to particulate concentrations (Lin et al., 2020). In contrast, data-driven approaches, including machine-learning (ML) and deep-learning (DL), learn direct mappings from image pixels or extracted features to $PM_{2.5}$ levels. Hybrid methods combine physically informed image features with ML or DL models to enhance predictive performance. The reported accuracy of

Figure 1. Comparison of saturation channel images: the left panel shows a clean-air scene, whereas the right panel depicts a polluted scene associated with high $PM_{2.5}$ concentration.

available methods varies widely depending on geographic context, seasonal conditions, image acquisition settings, and the availability of co-located PM measurements for training and validation.

With this in mind, we present the implementation of the AQpictures project (supported by the ISPRS Scientific Initiatives 2025, `https://www.isprs.org/society/si`), which aims to evaluate and compare image-based approaches for estimating PM concentrations in urban environments. The overarching objective is to develop an open, reproducible framework that enables the benchmarking, validation, and transferability of these methods across diverse urban contexts (see Figure 2). Specifically, the project focuses on (i) assessing the current state-of-the-art of image-based PM estimation, (ii) implementing the most representative methods by assessing them on test data, and (iii) deploying an open scientific toolkit, in the form of an open GitHub repository (`https://github.com/gisgeolab/aqpictures`), including sample data and source code, to support reproducibility and adaptation of these methods in different geographical and environmental settings.

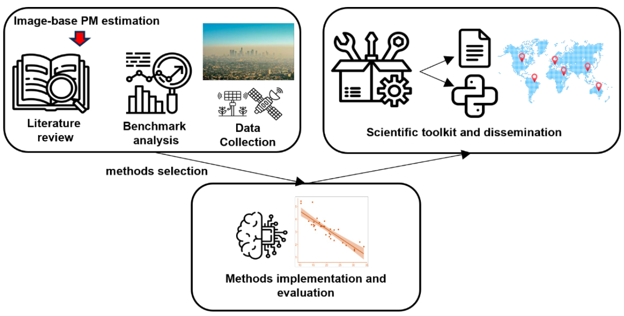

Figure 2. The AQpicture project workflow.

2. Literature Review Highlights

A literature review based on 46 studies published between 2014 and 2024 was conducted within the AQpictures project and is summarised here by reporting only the main findings. A comprehensive review article prepared by the authors is currently under consideration for journal publication. The full list of analysed studies is available in the project repository (`https://github.com/gisgeolab/aqpictures/tree/main/references`).

The review indicates that image-based estimation of ambient particulate matter, particularly $PM_{2.5}$, is emerging as a promising complementary approach to conventional air-quality monitoring, although the field remains relatively limited in scope and heterogeneous in methodology. Publication trends suggest a growing scientific interest in the use of outdoor imagery as a low-cost source of information for air pollution assessment. However, a strong geographical imbalance was identified, with most studies concentrated in East Asia, especially China, while other regions remain underrepresented. This limits the generalisability of current findings across diverse atmospheric, environmental, and urban contexts.

In terms of input data, fixed webcams and surveillance cameras are the most commonly used sources due to their stable viewpoints and continuous temporal coverage, whereas mobile and crowdsourced images are less frequently employed because of their higher variability in acquisition conditions. Ground-based monitoring stations are consistently used as reference data, often complemented by meteorological variables to improve model robustness. Image preprocessing (e.g., calibration, dehazing, segmentation) is widely applied, underlining its importance for reliable predictions.

From a methodological perspective, studies can be grouped into physics-based, ML, DL, and hybrid approaches. Physics-based models offer interpretability but are sensitive to atmospheric conditions, while ML methods provide moderate performance with lower computational cost. DL models generally achieve the highest predictive accuracy, with hybrid approaches representing a promising balance between robustness, interpretability, and performance. Quantitatively, DL reports the highest median performance ($R^2 > 0.90$), followed by hybrid, ML, and physics-based methods.

Model performance is strongly influenced by dataset size, environmental variability, and acquisition conditions, with reduced generalisability observed in heterogeneous urban contexts. This highlights the need for larger, multi-site, and multi-season datasets. Reproducibility also remains limited, as only a minority of studies provide open datasets and code, hindering systematic comparisons and validation. Overall, the review concludes that image-based PM estimation has significant potential as a complementary, low-cost monitoring approach, but further advances in data availability, model robustness, evaluation standardisation, and open-science practices are required to enable reliable and transferable applications.

3. Data and Methods

This section describes the data sources and methodological framework adopted in this study, building on the insights from the literature review to select and implement representative approaches from the main identified methodological families, including physics-based, ML, and DL models. Both the datasets and the source code of the methods described below are available in the project repository.

3.1 Data Collection

The study area is the city of Milan, located in the Lombardy region (northern Italy). Publicly accessible webcam locations were first compiled to identify potential image sources. As exact geographic coordinates were not available, approximate camera positions were inferred through visual inspection by identifying the most plausible installation points based on the scene content. Ground reference data were obtained from air-quality monitoring stations operated by ARPA Lombardia (https://www.arpalombardia.it/temi-ambientali/aria/rete-di-rilevamento), and each webcam was paired with the nearest station. Among the available candidates, the Milano MeteoGiuliacci webcam (https://www.meteogiuliacci.it/meteo-webcam/webcam-milano) was selected for the subsequent analysis.

Webcam imagery was acquired programmatically in Python using HTTP requests and HTML parsing. Image links were extracted from `<img>` tags and filtered to retain hourly snapshots, identified by filenames containing the string `hour`. The images were downloaded, organised into date-specific folders, and renamed following a consistent `YYYYMMDD-HHMM.jpg` convention. The analysis period spans January to October 2025; however, the archive is not continuous and includes temporal gaps due to the periodic execution of manual data collection routines. Meteorological and air-quality observations were retrieved from ARPA Lombardia, together with co-located meteorological variables. At the time of data collection, the 2025 observations had not yet undergone final quality control, which is typically completed in the following year. In addition, model-based predictors (air-quality and meteorological estimates at 0.1° resolution) were obtained from the Copernicus Climate Data Store and Atmosphere Data Store. For each dataset, the value of the grid cell corresponding to the webcam and ARPA station location was extracted and used in the analysis.

3.2 Physics-based Model

A Python-based workflow was developed to implement the methodology described in (Gu et al., 2018), aimed at deriving image-based indicators from fixed-camera sky imagery and relating them to hourly $PM_{2.5}$ observations. Image timestamps were extracted from filenames (format `YYYYMMDD-HHMM`) and used to temporally align image-derived features with corresponding ground-based $PM_{2.5}$ measurements, resulting in a synchronised labelled dataset.

For each image, a fixed region of interest was cropped to isolate the sky and remove non-relevant elements, ensuring consistency across the dataset. The cropped RGB image was then converted into a saturation map, which reduces sensitivity to absolute brightness while emphasising chromatic variability associated with atmospheric conditions. This representation was characterised using entropy-based descriptors. Two scalar features were extracted. The first, spatial entropy (H_S), was computed from the distribution of saturation values. The second, multiscale transform entropy (E_S), was derived using a wavelet-based decomposition to capture variability across spatial scales. Together, these features provide a compact description of image complexity potentially related to atmospheric turbidity. The resulting dataset consisted of timestamped records combining H_S, E_S, and $PM_{2.5}$ observations. To establish a reference baseline, clean-air Naturalness Statistics (NS) models were estimated by selecting samples with $PM_{2.5}$ concentrations below 12 μg/m^3 and fitting parametric distributions to the corresponding entropy features. A Gaussian model was used for H_S, while a Gumbel distribution was adopted for E_S. These baseline distributions provide a reference for identifying deviations from typical clear-sky conditions and support subsequent image-based air-quality interpretation.

3.3 Machine Learning Model

Following (Feng et al., 2021), a workflow was developed to extract compact colour descriptors from webcam images and combine them with atmospheric predictors for $PM_{2.5}$ estimation. Each image was processed as a three-channel RGB array and cropped to a fixed region of interest to ensure spatial consistency. The cropped image was then divided into two regions, representing the sky and the ground, and mean RGB values were computed for each region, resulting in a set of summary colour features.

These image-derived features were integrated with atmospheric predictors to construct the modelling dataset. Reanalysis variables (e.g., temperature, pressure, wind, and geopotential fields) were used to derive physically meaningful proxies, while colour-based indicators (e.g., channel ratios and brightness measures) were used to capture optical effects related to atmospheric scattering. Temporal information was incorporated through cyclical encoding of hour and month to represent diurnal and seasonal patterns. The modelling stage was based on the Classification and Regression Tree (CART) approach. To account for differences in illumination conditions, separate models were trained for daytime and nighttime data. $PM_{2.5}$ was used as the response variable, and the predictor set combined atmospheric, image-derived, and temporal features. After removing incomplete records, the dataset was split into training and testing subsets. Model complexity was controlled through a depth-sensitivity analysis, and predictive performance was evaluated using R^2, mean squared error (MSE), root mean squared error (RMSE), and observed-versus-predicted comparisons.

3.4 Deep Learning Model

A Multilayer Perceptron (MLP) model was implemented to predict ground-level $PM_{2.5}$, following the approach described in (Feng et al., 2021). The predictor set was consistent with that used in the machine-learning framework, combining atmospheric variables, image-derived features, and temporal descriptors.

Prior to training, input variables were normalised using min–max scaling to improve numerical stability and convergence. After removing incomplete records, the dataset was divided into training and testing subsets. A feed-forward MLP architecture with multiple hidden layers was trained to capture nonlinear relationships between predictors and $PM_{2.5}$. Model optimisation was performed over a fixed number of epochs using the Adam optimiser with mean squared error as the loss function. Training behaviour was monitored through the evolution of the loss function. Model performance was evaluated by comparing training and testing errors and analysing learning curves, enabling a consistent assessment of generalisation capability. This framework allows direct comparison between the MLP and CART models under the same experimental conditions.

4. Results

Considering the physics-based model, NS assumptions are only partly supported by the available data. In particular, the spatial entropy feature H_S shows an approximately unimodal and near-Gaussian distribution, with the fitted Gaussian model reasonably reproducing the main body of the empirical histogram. This indicates that H_S is relatively stable under low-PM conditions and can provide a plausible reference descriptor for clean-air scenes. By contrast, the transform entropy feature E_S displays a clearly skewed and heavy-tailed distribution, with an accumulation of high values that is not adequately captured by the fitted Gumbel model. This discrepancy suggests that the

https://doi.org/10.5194/isprs-archives-XLIX-B4-2026-563-2026 | © Author(s) 2026. CC BY 4.0 License.

parametric assumption adopted for E_S may be too restrictive, and that the resulting naturalness score may be affected by residual variability related to illumination, cloud conditions, or other heterogeneous sky states within the clean-air subset.

The observed-versus-predicted relationship further indicates that the physics-based style formulation has limited predictive capability in the present case. Predicted $PM_{2.5}$ values are concentrated within a relatively narrow interval despite a much broader range of observed concentrations, revealing weak sensitivity to actual pollution variability and poor responsiveness at higher $PM_{2.5}$ levels. This behaviour is consistent with the reported performance metrics, namely an MAE of approximately 10.79, an MSE of about 198.04, and an R^2 close to 0.03, all of which indicate that the model behaves similarly to a near-constant predictor rather than effectively reproducing event-scale changes in $PM_{2.5}$. Overall, these results suggest that the current entropy-based likelihood framework does not provide sufficient separation between clean and polluted conditions, and that the mapping from the naturalness indicator to $PM_{2.5}$ may be overly compressed or saturated. It should be noted, however, that these findings are based on a preliminary implementation and a relatively limited dataset, and therefore should not be considered conclusive. Further refinement of the modelling framework, together with more extensive and diverse training data, is required to fully assess the potential of this approach.

Moving to ML model results, the CART models showed very strong goodness of fit on the training data but only modest predictive skill on unseen samples, for both daytime and nighttime conditions. During the daytime, the fitted tree reached $R^2_{\mathrm{train}} = 0.948$ with $\mathrm{RMSE}_{\mathrm{train}} = 0.178$ on the log-transformed $PM_{2.5}$ values using $n_{\mathrm{train}} = 95$ samples. However, performance dropped markedly on the test set, where the model achieved only $R^2_{\mathrm{test}} = 0.209$ and $\mathrm{RMSE}_{\mathrm{test}} = 0.703$ over $n_{\mathrm{test}} = 42$ samples. This contrast indicates that the model was able to reproduce the structure of the training data well, but transferred only weakly to unseen daytime observations. The depth-sensitivity analysis shown in Figure 3 supports this interpretation, as training performance increased steadily with tree depth and approached a near-perfect fit, whereas testing performance improved only for relatively shallow trees and then became unstable, which is indicative of overfitting.

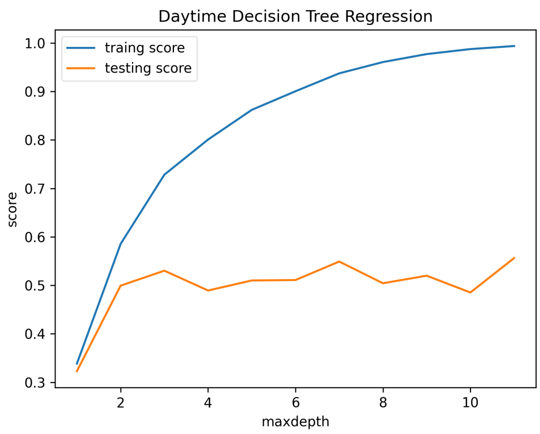

Figure 3. Daytime CART depth-sensitivity analysis: training and testing R^2 scores as a function of maximum tree depth.

The observed–predicted scatter plot in Figure. 4 provides further evidence of this behaviour, with training samples lying close to the 1:1 line and test samples showing a much wider dispersion, including several clear outliers. This suggests that the decision rules learned by the model are not sufficiently robust to generalise across unseen daytime conditions.

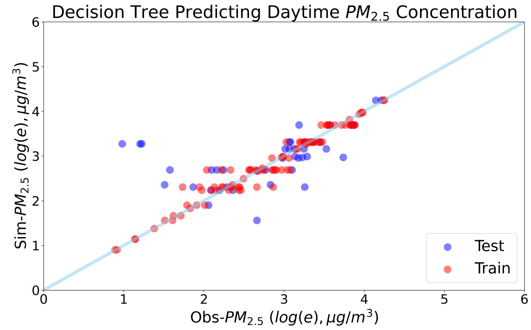

Figure 4. Daytime CART performance: observed vs. predicted $PM_{2.5}$ in log-space for training and testing samples. The solid line indicates the 1:1 relationship.

A similar pattern was observed for the nighttime model, although the tendency to overfit was even more pronounced. In this case, the CART model achieved an almost perfect fit on the training set, with $R^2_{\mathrm{train}} = 0.997$ and $\mathrm{RMSE}_{\mathrm{train}} = 0.041$ for $n_{\mathrm{train}} = 95$ samples. Despite this excellent in-sample performance, the predictive capability on the test set remained limited, with $R^2_{\mathrm{test}} = 0.201$ and $\mathrm{RMSE}_{\mathrm{test}} = 0.707$ based on $n_{\mathrm{test}} = 42$ samples. The depth analysis reported in Figure. 5 again showed that training scores rapidly converged toward 1 as tree complexity increased, while testing scores stayed low and fluctuated across the explored depths, again indicating poor generalisation.

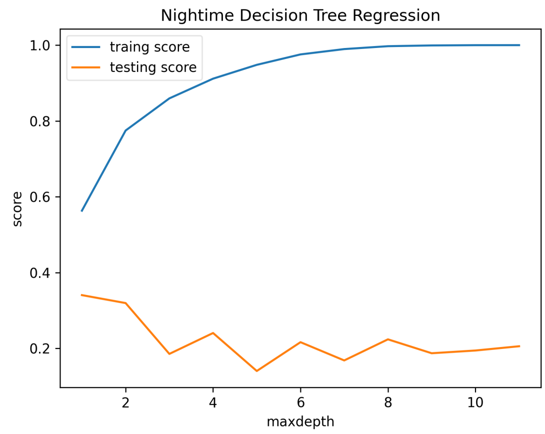

Figure 5. Nighttime CART depth-sensitivity analysis: training and testing R^2 scores as a function of maximum tree depth.

This behaviour is also visible in the nighttime observed–predicted scatter plot shown in Figure. 6, where the training cases cluster tightly around the 1:1 line, whereas the test cases are more widely scattered and include both underestimation and overestimation. Overall, these results suggest that, although the CART framework can capture complex patterns within the calibration data, its robustness on independent data remains limited under the current experimental setting.

Looking at the results of the preliminary implementation of the

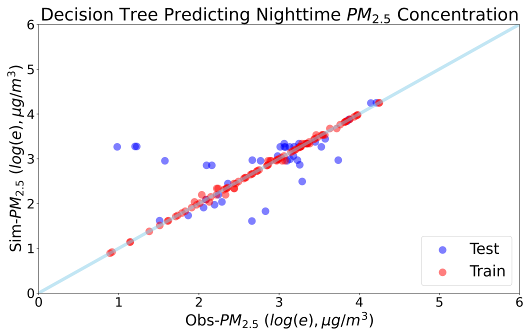

Figure 6. Nighttime CART performance: observed vs. predicted $PM_{2.5}$ in log-space for training and testing samples. The solid line indicates the 1:1 relationship.

DL method, the MLP model trained on the full dataset, including both daytime and nighttime observations, showed limited generalisation capability on the held-out test data. As illustrated by the learning curves in Figure. 7, the training mean squared error decreased progressively over the epochs, whereas the test mean squared error improved only during the initial training stage and then increased, which is indicative of overfitting. The final predictive performance on the test set remained weak, with an RMSE of 15.680 $\mu g/m^3$, an MAE of 13.005 $\mu g/m^3$, and a negative coefficient of determination ($R^2 = -3.046$). This result indicates that the model performed worse than a simple baseline based on the mean of the observations.

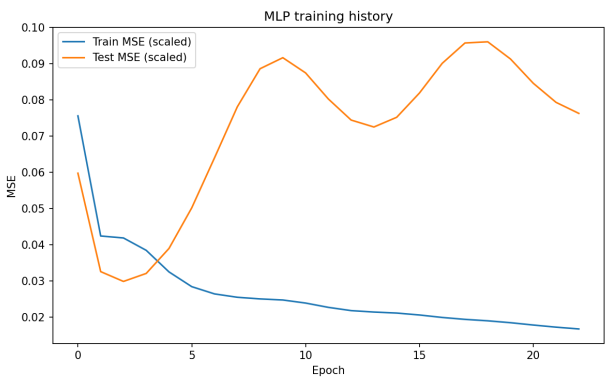

Figure 7. MLP training history: training and test MSE (scaled) as a function of epoch.

The observed–predicted comparison shown in Figure. 8 further confirms the limited predictive skill of the model. Rather than clustering around the 1:1 line, the predicted values are widely dispersed, and several cases show large deviations from the corresponding observations, including physically unrealistic negative estimates. This behaviour suggests that the nonlinear mapping learned by the network is unstable when daytime and nighttime regimes are merged into a single modelling framework. As with the other tested approaches, this result should be interpreted in light of the preliminary nature of the analysis and the limited size and heterogeneity of the available dataset, which may constrain the ability of data-driven models to learn robust and generalisable relationships. Additional model tuning, larger datasets, and more structured experimental configurations are needed before drawing definitive conclusions on model performance.

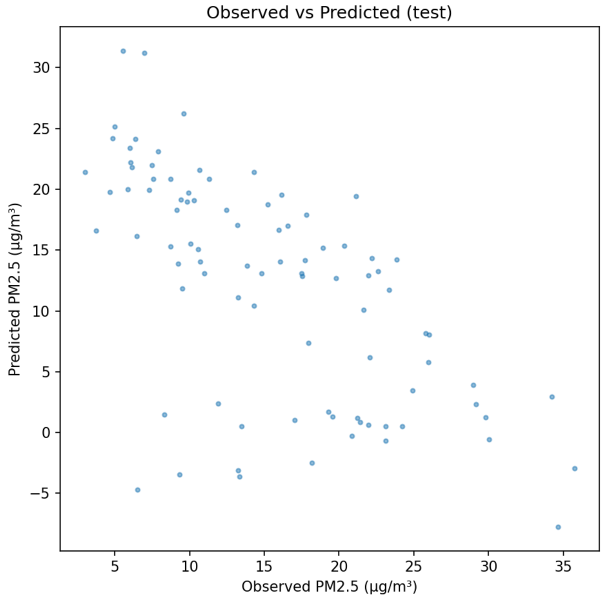

Figure 8. Observed versus predicted $PM_{2.5}$ concentrations on the test set for the MLP model. Predictions show a wide dispersion, with several large deviations from the observed values, including physically unrealistic negative estimates.

5. Conclusion and Future Work

This work presented the AQpictures project as an initial effort to assess the potential of image-based methods for $PM_{2.5}$ estimation using outdoor imagery and openly reproducible workflows. By combining a structured literature review with an initial experimental benchmark in Milan, the study provides both a synthesis of the current state of research and a practical test of representative modelling approaches under a common case-study framework. Overall, the project confirms that webcam imagery can represent a valuable low-cost complementary source of information for air-quality analysis, while also showing that reliable $PM_{2.5}$ estimation from outdoor images remains a challenging task that is strongly dependent on data quality, environmental variability, and modelling choices.

The literature review highlighted a rapidly growing but still methodologically fragmented research field and limited reproducibility due to the scarce availability of open datasets and source code. Within this context, the Milan benchmark enabled the implementation and comparison of representative physics-based, ML, and DL approaches. The tested models showed limited generalisation capability, with machine-learning regression achieving high in-sample performance but substantially lower predictive skill on testing data, while the other approaches exhibited generally weak or unstable performance.

Beyond these quantitative results, the benchmark was particularly valuable in identifying the main practical challenges affecting image-based $PM_{2.5}$ estimation. These include sensitivity to illumination regimes, limited transferability across conditions, overfitting in data-driven models, and the difficulty of deriving stable image-to-pollution relationships from relatively small and heterogeneous datasets.

From this perspective, the main outcome of the AQpictures project is not only the preliminary assessment of specific models, but also the definition of a reproducible benchmarking workflow that can support future comparative analyses. The study helped clarify which aspects of the modelling chain require the greatest attention, including data collection, image preprocessing, temporal alignment, feature design, model calibration, and validation strategy. It also confirmed the importance of integrating image-derived variables with ancillary meteorological information, and of explicitly accounting for differences between daytime, nighttime, and possibly transitional illumination conditions.

Several directions for future work therefore emerge from this initial phase. First, the dataset should be expanded and diversified to better represent seasonal, meteorological, and illumination-related variability, ideally through multi-camera and multi-site experiments. Second, validation strategies should move towards more realistic time-aware schemes in order to better assess model transferability across periods and conditions. Third, model development should include stronger regularisation, more systematic hyperparameter tuning, and the testing of more robust learning frameworks, including ensemble and hybrid approaches. Additional effort is also needed in feature engineering, for example by incorporating cloud conditions, solar geometry, haze-sensitive image descriptors, and potentially satellite-derived variables as complementary predictors. For physics-based methods, more flexible statistical assumptions and alternative formulations should also be explored.

More broadly, the project underlines the need for standardised and openly accessible benchmarking practices in this field. In line with this objective, the workflows and sample datasets developed in AQpictures will be progressively released and extended through the project GitHub repository (`https://github.com/gisgeolab/aqpictures`), to support reproducibility, facilitate method comparison, and enable future applications in broader geographical contexts. Taken together, the results of this work suggest that image-based $PM_{2.5}$ estimation should currently be regarded as a complementary rather than substitute monitoring strategy, but one with significant potential for future development if supported by larger datasets, more rigorous validation, and open collaborative research practices.

Acknowledgements

This work has been supported by the Scientific Initiatives 2025 (`https://www.isprs.org/society/si`) of the International Society for Photogrammetry and Remote Sensing (ISPRS).

References

Chen, Q., Chen, W., Pan, G., 2022. An improved picture-based prediction method of $PM_{2.5}$ concentration. *IET Image Processing*, 16(11), 2827–2833.

Feng, L., Yang, T., Wang, Z., 2021. Performance evaluation of photographic measurement in the machine-learning prediction of ground $PM_{2.5}$ concentration. *Atmospheric Environment*, 262, 118623.

Fowler, D., Brimblecombe, P., Burrows, J., Heal, M. R., Grennfelt, P., Stevenson, D. S., Jowett, A., Nemitz, E., Coyle, M., Liu, X. et al., 2020. A chronology of global air quality. *Philosophical Transactions of the Royal Society A*, 378(2183), 20190314.

Gu, K., Qiao, J., Li, X., 2018. Highly efficient picture-based prediction of $PM_{2.5}$ concentration. *IEEE Transactions on Industrial Electronics*, 66(4), 3176–3184.

He, Z., Ye, X., Gu, K., Qiao, J., 2018. Learn to predict $pm_{2.5}$ concentration with image contrast-sensitive features. *2018 37th Chinese Control Conference (CCC)*, IEEE, 4102–4106.

Lin, F.-C., Lu, S.-H., Liang, C.-J., Chen, Y.-H., Liang, J.-J., 2020. Quantifying source apportionment for ambient haze: An image haze extraction approach with air quality monitoring data. *Environmental Research*, 184, 109216.

Liu, C., Tsow, F., Zou, Y., Tao, N., 2016. Particle pollution estimation based on image analysis. *PloS one*, 11(2), e0145955.

Sloss, L. L., Smith, I. M., 2000. PM_{10} and $PM_{2.5}$: an international perspective. *Fuel Processing Technology*, 65, 127–141.

Wang, G., Shi, Q., Wang, H., Sun, K., Lu, Y., Di, K., 2022. Multi-modal image feature fusion-based $PM_{2.5}$ concentration estimation. *Atmospheric Pollution Research*, 13(3), 101345.

Wang, X., Wang, M., Liu, X., Mao, Y., Chen, Y., Dai, S., 2024. Surveillance-image-based outdoor air quality monitoring. *Environmental Science and Ecotechnology*, 18, 100319.

Yao, S., Wang, F., Huang, B., 2022. Measuring $PM_{2.5}$ concentrations from a single smartphone photograph. *Remote Sensing*, 14(11), 2572.

Yue, G., Gu, K., Qiao, J., 2019. Effective and efficient photo-based $PM_{2.5}$ concentration estimation. *IEEE Transactions on instrumentation and measurement*, 68(10), 3962–3971.